Answer to the reviewers on the manuscript:
"Light-coupled cryogenic probes to detect low micromolar samples and allow automated NMR platform"

We thank the reviewers for their careful reading and overall positive appreciation. The comments and suggestions improve the quality of the presented work and increase the value delivered to the community.

Referee 1:

Nice work. Well written manuscript. Should be published with the following corrections.

Figure 1 caption, last line: "function of lateral axial distance"?

We thank Referee 1 for the careful reading, and we corrected the typo in the caption of figure 1.

"E) Simulation of the absorbed power (AU) in the NMR sample volume as a function of lateral axial distance (Lateral y shift) for different NA values and optic fiber diameters (500 and 900 µm)."

Line 108: "the insertion of the optic fiber has no impact on the field homogeneity caused by inserting an optical fiber" – unnecessary repetition.

We thank Referee 1 for the careful reading and corrected the sentence for better readability.

"To verify the absence of field homogeneity perturbation caused by inserting an optical fiber close to the B_1 coils, we recorded the spectra of 0.3% $CHCl_3$ in acetone-d_6, the standard line shape reference sample (Figure 2A)."

Line 137: Figure 3 (not 2).

We thank Referee 1 for the careful reading and we corrected the Figure number in reference to Figure 3.

Line 141 and elsewhere: the author of the article referred to as "In Bonn, 1954" is August Beer (of the Beer-Lambert Law) working at the University of Bonn.

We thank Referee 1 for the careful reading, we corrected manually the references in our reference manager software. The reference now reads "Beer, 1852".

Line 154: define the STD abbreviation

We thank Referee 1 for noticing the absence of a definition for this acronym. It is now corrected in the main text.
"Such concentrations are on the low standard of typical fragment screening by NMR; for saturation transfer difference (STD) NMR screening, the ligand concentrations vary between 50 to 500 µM."

Line 174: spherical bottom?

Indeed, we thank Referee 1 for noticing the typo.

Line 204: shouldn't KPO4 be K3PO4 or K2HPO4 or KH2PO4?

KPO4 is a commonly used abbreviation for phosphate salts with potassium counter ion, the exact protonation mix depends on the pH. Nevertheless Referee 1 is right, this is an inexact notation. To avoid confusion we rewrote KPO4 as "potassium phosphate buffer."

The list of references has been carelessly compiled: missing page numbers, incomplete author lists, acronyms in sentence case, "in Bonn, B".

We thank Referee 1 for bringing this mistake to our attention. We made a mistake with our reference manager software. We corrected the references manually.

“Bargon, J. and Fischer, H.: Kernresonanz-Emissionslinien Wahrend Rascher Radikalreaktionen .2. Chemisch Induzierte Dynamische Kernpolarisation, Zeitschrift für Naturforschung A, 22, 1556-1562, 1967.
Becker, M., Lehmkuhl, S., Kesselheim, S., Korvink, Y., Jouda, M.: Acquisitions with random shim values enhance AI-driven NMR shimming, Journal of Magnetic Resonance, 345, 107323, 2022.
Beer, A.: Bestimmung der Absorption des rothen Lichts in farbigen Flüssigkeiten, Annalen der Physik, 162, 78-88, 1852.
Bodenhausen, G. and Ruben, D. J.: Natural Abundance N-15 NMR by Enhanced Heteronuclear Spectroscopy, Chemical Physics Letters, 69, 185-189, 1980.
Bramham, J. E. and Golovanov, A. P.: Sample illumination device facilitates in situ light-coupled NMR spectroscopy without fibre optics, Communication Chemistry, 5, 90, 2022.
Closs, G. L.: A Mechanism Explaining Nuclear Spin Polarizations in Radical Combination Reactions, Journal of the American Chemical Society, 91, 4552-4554, 1969.
Dixon, J. M., Taniguchi, M., and Lindsey, J. S.: PhotochemCAD 2: a refined program with accompanying spectral databases for photochemical calculations, Photochem Photobiol, 81, 212-213, 2005.
Greivenkamp, J. E.: Field Guide to Geometrical Optics, SPIE., 2004.
Hore, P. J. and Broadhurst, R. W.: Photo-CIDNP of Biopolymers, Progress in Nuclear Magnetic Resonance Spectroscopy, 25, 345-402, 1993.
Kaptein, R. and Oosterhoff, L. J.: Chemically induced dynamic nuclear polarization III (anomalous multiplets of radical coupling and disproportionation products), Chemical Physics Letters, 4, 214-216, 1969.
Kerber, P. J., Nunez, R., Jensen, D. R., Zhou, A. L., Peterson, F. C., Hill, R. B., Volkman, B. F., and Smith, B. C.: Fragment-based screening by protein-detected NMR spectroscopy, Methods in Enzymology, 690, 285-310, 2023.
Koeppe, B., Tolstoy, P. M., and Limbach, H. H.: Reaction pathways of proton transfer in hydrogen-bonded phenol-carboxylate complexes explored by combined UV-vis and NMR spectroscopy, Journal of the American Chemical Society, 133, 7897-7908, 2011.
Kuhn, L. T.: Photo-CIDNP NMR spectroscopy of amino acids and proteins, Topics in Current Chemistry, 338, 229-300, 2013.
Kuhn, L. T., Weber, S., Bargon, J., Parella, T., and Perez-Trujillo, M.: Hyperpolarization-Enhanced NMR Spectroscopy of Unaltered Biofluids Using Photo-CIDNP, Analytical Chemistry, 96, 102-109, 2024.
Kuprov, I. and Hore, P. J.: Uniform illumination of optically dense NMR samples, Journal of Magnetic Resonance, 171, 171-175, 2004.
Morozova, O. B. and Ivanov, K. L.: Time-Resolved Chemically Induced Dynamic Nuclear Polarization of Biologically Important Molecules, Chemphyschem, 20, 197-215, 2019.
Okuno, Y. and Cavagnero, S.: Fluorescein: A Photo-CIDNP Sensitizer Enabling Hypersensitive NMR Data Collection in Liquids at Low Micromolar Concentration, The Journal of Physical Chemistry B, 120, 12416-12416, 2016.
Sobol, A., Torres, F., Aicher, A., Renn, A., and Riek, R.: Atto Thio 12 as a promising dye for photo-CIDNP, The Journal of Chemical Physics, 151, 234201, 234201, 2019.
Stadler, G. R., Segawa, T. F., Butikofer, M., Decker, V., Loss, S., Czarniecki, B., Torres, F., and Riek, R.: Fragment Screening and Fast Micromolar Detection on a Benchtop NMR Spectrometer Boosted by Photoinduced Hyperpolarization, Angewandte Chemie International Edition, 62, e202308692, 2023.
Taniguchi, M., Du, H., and Lindsey, J. S.: PhotochemCAD 3: Diverse Modules for Photophysical Calculations with Multiple Spectral Databases, Photochemistry Photobiology, 94, 277-289, 2018.
Tolstoy, P. M., Koeppe, B., Denisov, G. S., and Limbach, H. H.: Combined NMR and UV/vis spectroscopy in the solution state: study of the geometries of strong OHO hydrogen bonds of phenols with carboxylic acids, Angewandte Chemie International Edition, 48, 5745-5747, 2009.
Torres, F., Sobol, A., Greenwald, J., Renn, A., Morozova, O., Yurkovskaya, A., and Riek, R.: Molecular features toward high photo-CIDNP hyperpolariztion explored through the oxidocyclization of tryptophan, Physical Chemistry Chemical Physics, 23, 6641-6650, 2021.
Torres, F., Bütikofer, M., Stadler, G. R., Renn, A., Kadavath, H., Bobrovs, R., Jaudzems, K., and Riek, R.: Ultrafast Fragment Screening Using Photo-Hyperpolarized (CIDNP) NMR, Journal of the American Chemical Society, 145, 12066-12080, 2023.
Torres, F., Renn, A.; Riek, R.: Exploration of the close chemical space of tryptophan and tyrosine reveals importance of hydrophobicity in CW-photo-CIDNP performances, Magnetic Resonance, 2, 321-329, 2021.
Ward, H. R. and Lawler, R. G.: Nuclear Magnetic Resonance Emission and Enhanced Absorption in Rapid Organometallic Reactions, Journal of the American Chemical Society, 89, 5518-5519, 1967.

Williamson, M. P.: Using chemical shift perturbation to characterise ligand binding, Progress in Nuclear Magnetic Resonance Spectroscopy, 73, 1-16, 2013.
Yang, H. M., Li, S. Y., Mickles, C. A., Guzman-Luna, V., Sugisaki, K., Thompson, C. M., Dang, H. H., and Cavagnero, S.: Selective Isotope Labeling and LC-Photo-CIDNP Enable NMR Spectroscopy at Low-Nanomolar Concentration, Journal of the American Chemical Society, 144, 11608-11619, 2022.
”

And in the *Supplementary Information*

Page 1: the title doesn't match that of the main text.

We thank Referee 1 for bringing this mistake to our attention. We corrected the title.

Figure S2: “a 3mm NMR tube with lensed bottom with lensed bottom” – too many bottoms.

We corrected the caption which now reads:
“Figure S2: Microscopic photograph of a 3mm NMR tube with lensed bottom. This lens shape is usually present in standard tubes. The two circles define the two curvatures of the convex lens.”

Figure S2: The labelling of the figure would be easier to read if it were higher resolution.

We provided the high-resolution image of Figure S2.

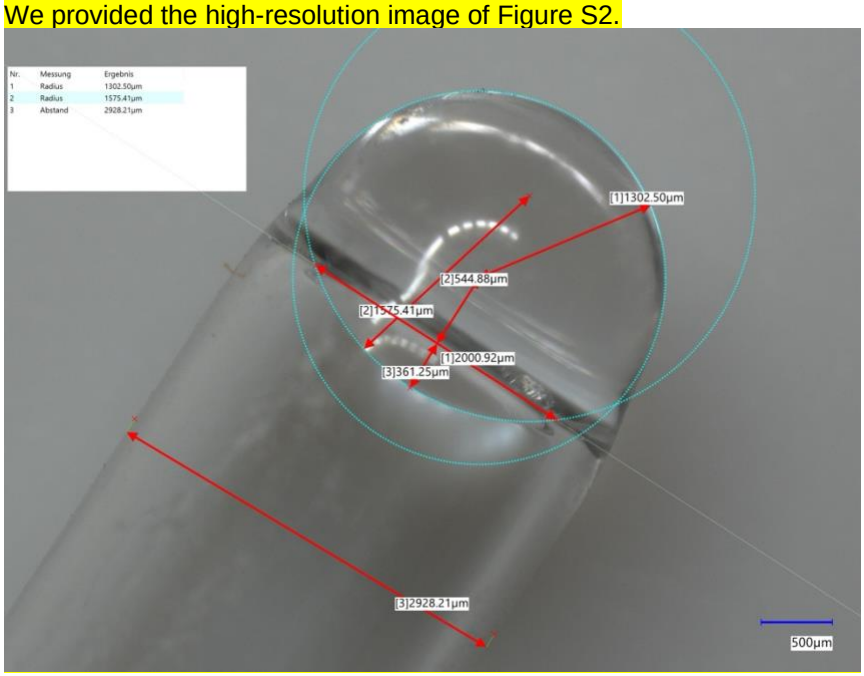

Figure S3: At first glance, there appears to be very little difference between the three photographs. Is that the point? It would be helpful if the caption could explain things a bit more.

We thank Referee 1 for bringing this to our attention. We modified figure 2 to provide zoom on the tubes exhibiting, hence, the different light path: diverging, collimated, and converging. Figure S3 and its caption now reads:

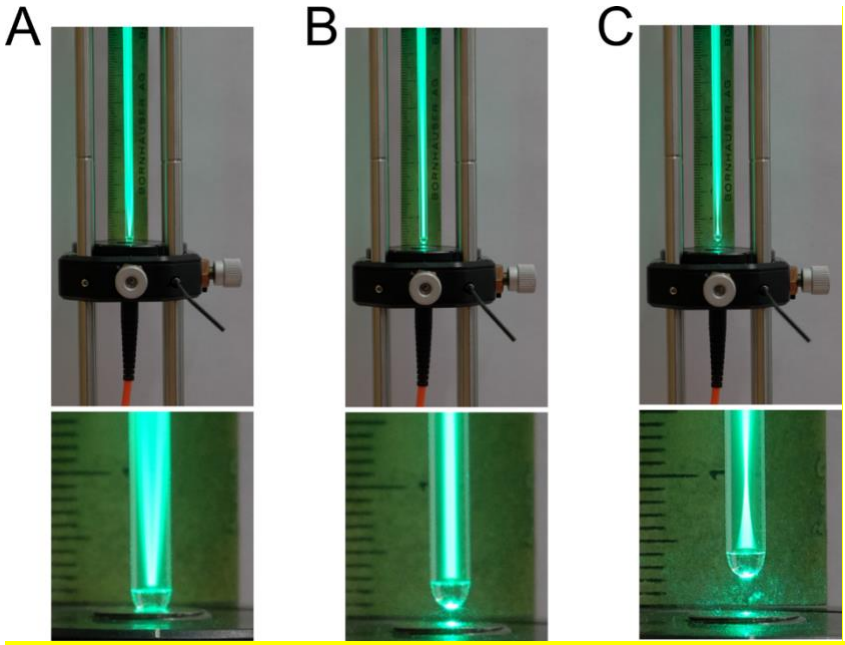

Figure S3: Benchtop experiment with a fiber NA=0.22 and a 3mm NMR tube. The fiber is positioned at different distances along the z-axis from the NMR tube. In all cases the light is guided within the sample liquid and NMR glass tube walls via total internal reflection (top part of the figure) Depending on the offset distance, the beam has different shapes after entering the liquid sample (bottom part of the figure: zoom-in of the top around the light entrance). A) Offset: 0.0 mm – the beam is initially divergent B) Offset: 1.0 mm – the beam is initially collimated C) 2.5 mm – the beam is initially focused.

Referee 2:
The manuscript by Wüster et al titled “An automated NMR platform with light-coupled cryogenic probes to detect low micromolar samples” describes an approach to how sample illumination using optical fiber can be embedded in a cryoprobe using an existing inside channel normally used for flow-cell accessory. The other end of the optical fiber can be coupled, as usual, to a laser or a laser diode. Light enters through the bottom of the NMR sample tube via an effective lens formed by the tube bottom, and if the optical density of the sample is not very high, the light then penetrates the sample and illuminates the NMR detection area. The main benefit of this approach is that it leaves the top of the magnet bore completely opened so that the sample lift and automatic sample changers can operate as usual, meaning that full sample automation present nowadays on modern NMR spectrometers can be fully operational, and be applied to samples under illuminated conditions. Overall it is a very clever way to introduce the illumination to the bottom of the sample from within the probehead itself, yet without any probehead modification, apart from routing the optical fiber through the existing channel. Such positioning of the fiber does not noticeably compromise shimming, signal lineshape, or other characteristics of the probe, as the authors demonstrate in their manuscript. From this viewpoint, the submitted paper will be undoubtedly useful for the community that aims to couple sample illumination with NMR spectroscopy, and moreover, will likely trigger follow-on studies where this approach will be further modified, optimized and improved. However, before accepting this manuscript for formal publication a few things should be done to make sure that this paper lays a robust foundation for this approach and can be used as a guide by others.
1) it will be perhaps interesting for the community if there is a short discussion included of whether all the Cryoprobes, or only specific types, have this port for the flow-probe accessory, and some discussion of usability of 5 mm vs 3 mm cryoprobes and sample tubes. The exact type of cryoprobe used in the study is not mentioned, unfortunately, only the spectrometer used. It is not clear if this was 5mm cryoprobe, or 3mm cryoprobe.

We thank Referee 2 for this comment. Indeed, we included in the material and method the cryoprobe that we used to install our setup.

“All NMR measurements were performed at 298 K on a Bruker Avance III HD 600 MHz spectrometer equipped with a Bruker TCI 600 $^{1}H/^{13}C/^{15}N$ MHz CryoProbe.”

In addition, we commented on the compatibility of our setup in the discussion.

“Such port is accessible in all 5-mm standard CryoProbes (but not for 3mm and 1.7mm CryoProbes) as well as Prodigy CryoProbes from 300 MHz-900 MHz.”

2) the title of the paper has somewhat imprecise wording at the very beginning if one considers what data is actually included in the manuscript itself. The title implies that “an automated NMR platform” was presented in the paper, but automation as a platform was not demonstrated here, just the illumination approach. We suggest modifying the title slightly (along the lines that the approach "*allows* automation") so it reflects more precisely the actual data included in the paper. (As another Review already noted, in the Supplemental the title is actually very different.) In the Discussion/Conclusions it is of course fair to say that this approach would be fully compatible with automation, no doubt about that.

Thank you for noticing the error in the supplementary title. We corrected the main title in alignment with the suggestion. The title in the supplementary was corrected accordingly. As a side note for the interest of the referee, we have now implemented the system presented here on an NMR spectrometer equipped with SampleJet.

3) the paper presents results of simulations and ray tracing, which is good for displaying that light will go inside the sample and be largely confined within the sample and the sample tube. However, the most interesting things, like the effects of light absorbance in the sample and light scattering are not described in enough detail. What will change in light distribution if 5 mm tube is used instead of 3 mm tube? (There may be more 5 mm cryoprobes around than 3mm cryoprobes, I suspect, and 5 mm tubes are common). It is mentioned in the Conclusion (line 193) that “we built setup that illuminated 3mm *and 5mm NMR tubes*” but no data was shown in the paper regarding 5mm tubes, so either the data for 5mm tubes needs to be added

Referee 2 is correct. This setup can be used for 5 mm tubes. However, we focus on 3mm tubes as they are the most commonly used in drug discovery applications to save on the quantity of recombinant protein necessary to perform all screening. To ensure the completeness of the present scientific report, we provided more information in supplementary material.

"The optic fiber-coupled cryogenic probes are also compatible with standard 5mm tubes. Figure S5 shows a 5 mm tube illuminated with an NA=0.22 fiber for two longitudinal offsets. The working principle is the same. Depending on the longitudinal offset, the homogeneity of the light in the NMR active region can be optimized.

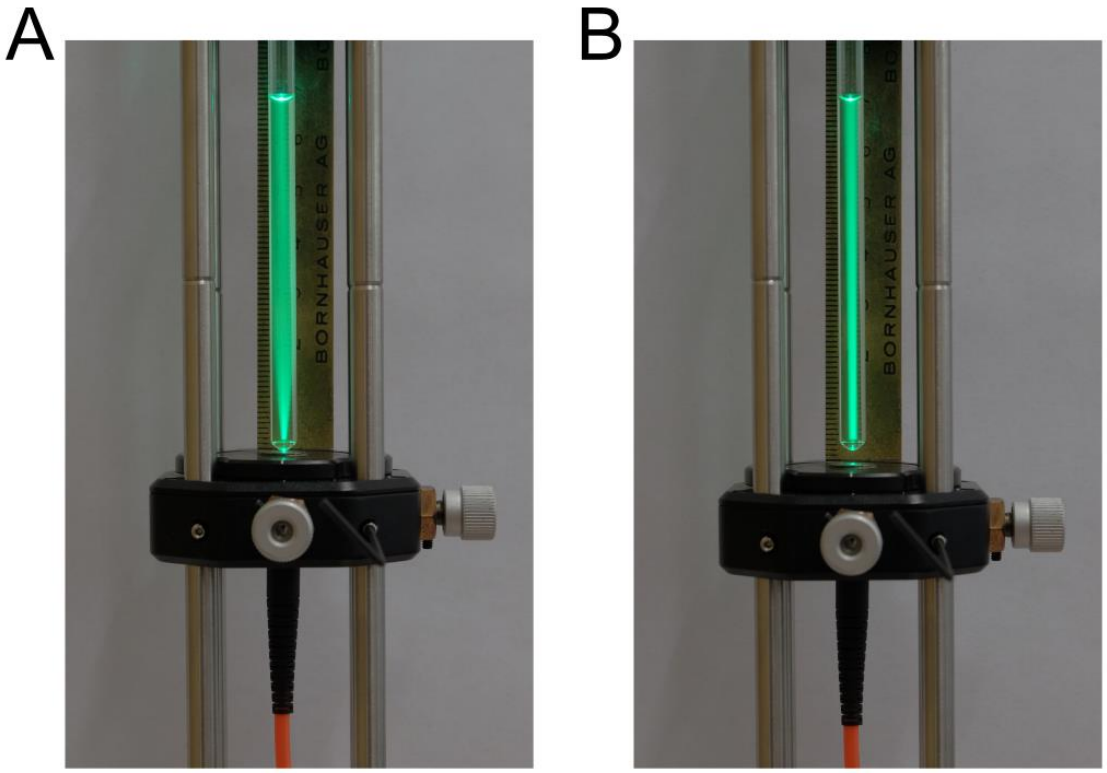

Figure S5: Optical Bench Top experiment of a 5mm NMR tube with lensed bottom illuminated by a NA=0.22 optical multimode fiber. A) Longitudinal offset: 0 mm. Here the beam is initially divergent and the light in the NMR active region illuminates the whole sample volume. B) Longitudinal offset: 2.5 mm. Here, the light beam is collimated, and only part of the sample volume is illuminated."

We referred to the supplementary material in the main text:
"This allows the irradiation of the samples contained in standard 3 mm and 5 mm NMR tubes from the bottom (Figure S5), taking advantage of the spherical bottom and resulting in a lensing effect."

, or claim "we built setup that illuminated […] *5mm* tubes" modified. Presumably, in 5mm tubes there will be more unlit areas close to the tube walls towards the bottom half of the sample, where the beam enters, but how bad the situation might be is not really obvious without a simulation and/or experimentation. Moreover, ray tracing (presumably?) would not account for light absorbance and scattering within the sample and within the tube walls, but that is what ultimately defines the distribution of light in the NMR active volume, and in the sample in general.

We thank Referee 2 for carefully considering the different parameters. However, the ray tracing simulation does account for absorbance within the sample. Each ray is attenuated while traveling through the absorptive medium using the Beer-Lambert law. Scattering is neglected, as it is assumed to have a minor influence. We modified the material and methods to provide more complete information to readers who might share similar concerns:

"For the optical simulations, Ansys Zemax OpticStudio was used in non-sequential mode. The software performs a Monte Carlo simulation by computing the path of many randomized light rays through the geometry modeled according to the experimental setup. The simulation accounted for the

absorption, which was set to agree with the media's optical density (OD), and the scattering was neglected as it is expected to have a minor influence.
”

The authors do mention (lines 197-198) that it is “possible to detect power levels at different axial positions within the liquid sample using an immersed photodiode”, however, this experimental data on such measurements is not shown anywhere, and is certainly worth adding.

We thank Referee 2 for this remark. Indeed, we should have provided details on this particular point. We added the corresponding figure in the supplementary. For Referee 2's interest in drug discovery applications involving a low concentration of small molecules, the typical concentration of the photosensitizer is between 2 and 10 µM. As one can notice,60% of the power is retained even at concentrations that are in the high standard for drug discovery (20%).

“In order to get an experimental estimate on the absorbed optical power as function of the position in the liquid sample, we immersed a photodiode inside of the sample for four different fluorescein concentrations. We used the recorded power levels at 0 µM (distilled water) as reference value and normalized all powers to these reference powers, see Figure S6.

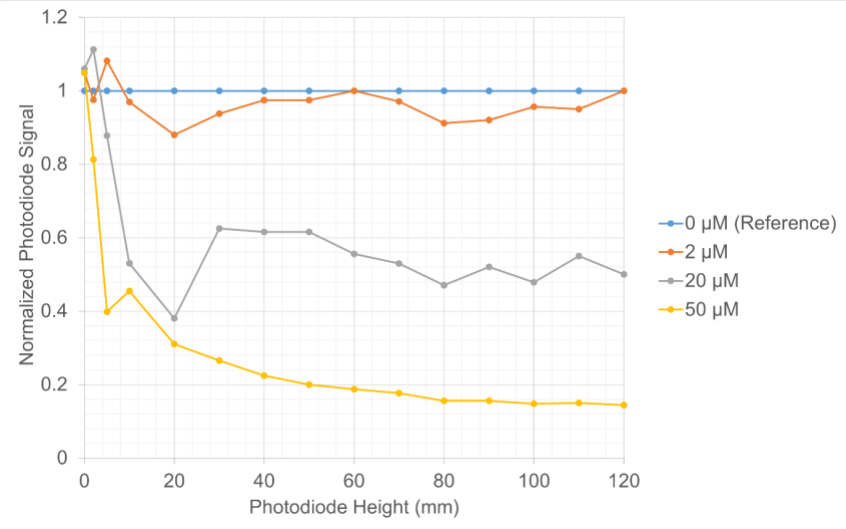

Figure S6: Normalized power level on photodetector as a function of height in the NMR liquid sample tube. The position of 0 mm corresponds to the photodiode at the bottom of the tube. The Fluorescein concentrations vary between 0 µM and 20 µM, and the power levels remain high (approximately 60%) for different heights of the photodiode position. For high concentrations of 50 µM and higher, we see a significant drop in the power levels due to high light absorption in the sample.”

How uniformly the sample is illuminated in reality would be of great importance to many, if this approach is to be used as a “platform”. Apart from using a photodiode for ex-situ measuring using the model benchtop rig (Fig1C), it would be really useful to measure the experimental light uniformity inside the sample in the cryoprobe (with all the sample tube surroundings present there).

We thank the referee for the thoughts about light uniformity inside the sample and within the cryoprobe surroundings. We think that the surrounding of the cryoprobe will not change the results since the light is confined to the sample via total internal reflection, but it is correct that the positioning of the fiber within the cryoprobe is not as rigid as on a benchtop setup, and might have an effect on the light uniformity. To further elucidate the question of light uniformity, we will include a z-dependent absorption simulation. We make a statement in the main text.

“Optimizing the photosensitized concentration can also improve the homogeneity of the illumination and maximize the photo-CIDNP hyperpolarization (Figure S7).”

We will add the following figure and text to the supplementary material:

“In Figure S7 we calculated the z-position-dependent absorbed light within the NMR sample. We find that for fluorescein concentrations around 20 µM, we can expect the largest photo-CIDNP signal, which will drop towards lower and higher concentrations.

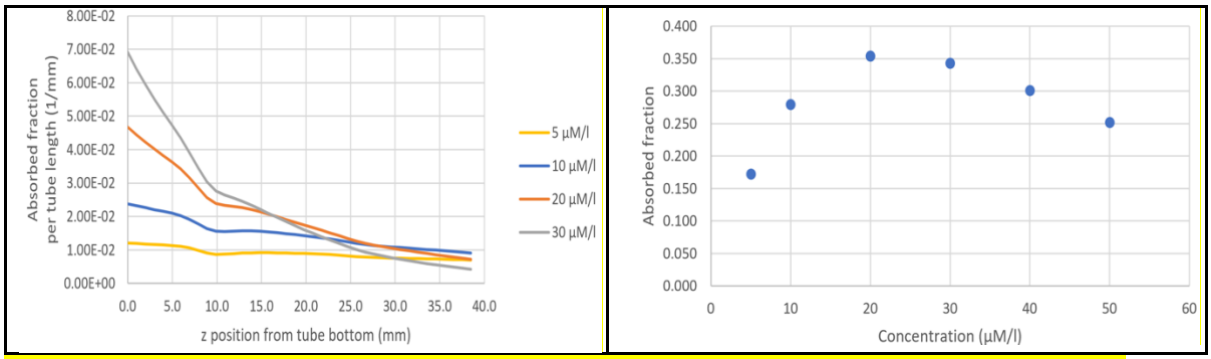

Figure S7 Left: Simulation of the absorbed light by the sample per tube length for different fluorescein concentrations. Right: Absorbed light within the NMR active volume vs. Fluorecein concentration. At 20 µM concentration, most light is absorbed, but the sample volume is illuminated more uniformly at lower concentrations.
Tube diameter: 3 mm, Fiber distance to tube: 2 mm, Fiber NA: 0.22, Fiber diameter: 0.9 mm.”

Presumably, this can be done using slice-selective photo-CIDNP, or slice-selective reaction with some suitable actinometer, or just using Z-position-dependent photo-CIDNP enhancement factor using imaging experiment for illuminated and dark z-profiles, and dividing one by another (like it was done for NMRtorch in Bramham and Golovanov, Comm Chem, 5, 2022; very easy if photo-CIDNP enhancements are high enough). This will quantify the real *absorbed* light intensity distribution along the length of the sample inside the NMR active volume inside the spectrometer.

We appreciate the reviewer's suggestion regarding the use of slice-selective photo-CIDNP measurements. This will be certainly something we would like to perform in future studies. While we did not employ this technique in our current manuscript, we opted for two complementary methods. 1.) Ray tracing simulation 2.) Immersed photodiode measurement to quantify light intensity distribution within the sample. For the simulation results, we find that the absorbed light drops to a percentage of 65 percent of the initial light power (lambda = 450nm) at the beginning of the active NMR region (after 10 mm travel distance) and a further decrease to 46 percent at the end of the NMR active region (after 30 mm travel distance) for the 10 µM fluorescein sample. For the immersed photodiode measurement, we find a similar behavior as in the simulation, and we conclude that we have sufficiently large power levels for photo-CIDNP experiments at typical concentrations between 2 uM and 20 uM.

On line 95 the claim is made that “inserting the optical fiber near NMR tube *yields high illumination* of the sample”, however, what is considered as “high illumination” is a bit vague, it is only compared with the illumination from the top, and looks a bit worse, for the reasons outlined in the paper. Either the statement needs to be somewhat reworded, or some quantification shown.

Referee 2 is correct. At this point in the manuscript, it is not clear that we achieve high illumination. However, later (Line 137 to 173) we clearly demonstrate that the anomalous line intensities are 80% as intense as for the classic setup involving an optic fiber dipped into the liquid sample. This illumination enables the detection of low µM concentration within a single scan with an excellent signal-to-noise. The simulations, as described in the same section show that the setup yields high illumination—according to our simulation, roughly 9% of the incident light on the NMR tube is lost via Fresnel reflection when transmitted through the NMR tube glass, and absorption is the cause of the rest of the very acceptable difference in illumination between the two setups.
Nevertheless, we rephrased our statement:

"In summary, these results support our experimental findings that inserting the optical fiber near the NMR tube yields illumination of the sample in the NMR tube."

Further discussion will be useful in the paper as to what may be the maximal sample optical density where the light penetration and light uniformity in the NMR detection region will be still satisfactory. The current arrangement (Fig1C) implies that only a small amount of light is absorbed by the sample, and the major part just passes through, reducing the illumination efficiency. It is mentioned in the paper that a simple way to improve photo-CIDNP hyperpolarization could be to use stronger laser power (line 153), but this will not improve light uniformity and may induce local heating and excessive dye bleaching at the point where the beam enters the sample,

Referee 2 is right: the laser power will cause more bleaching, and this option would only be useful for single-scan experiments, such as screening.

"Therefore, a simple way to improve the photo-CIDNP hyperpolarization could be to use stronger laser powers to compensate for the optical density and the Fresnel reflection. However, this would yield more photosensitizer bleaching and should only be considered for the single or low number of scan applications."

not to mention that higher laser power may be degrading the optical fiber itself. All these issues should be mentioned or discussed in the paper, or, even better, at least some of these effects measured (ideally).

Referee 2 is correct is absolute, but not in the condition that we use in this article. This is essentially the case for wavelengths in the UV. According to the Thorlabs website practical safe power limits for optical silica fibers are on the order of 250 kW / cm^2 – this translates to a power limit of roughly 1.6 kW for a 900 µm diameter multimode fiber. We are 3 order of magnitudes below this value. https://www.thorlabs.com/NewGroupPage9_PF.cfm?ObjectGroup_ID=362

Another thing – it is fairly easy to position the end of the fiber at the very bottom of the sample tube in the open desktop rig used for testing (Fig1C), however inside the cryoprobe the bottom of the sample tube is not visible, and the tube position in the spinner is normally set by an external gauge and is not really movable. Some tips or comments would be useful to advise how the recommended small optimal distance between the end of the fiber and the tube bottom can be set inside the cryoprobe where both of these things are not visible.

We added in the Material and Method the procedure to insert the optic fiber. As reads below:

"The fiber is inserted from the entry of the air conduct, which is typically connected to the BCU. The connection to the BCU is maintained using a T-connector to accommodate the optic fiber and the BCU tubing. The fiber is inserted until the user feels the resistance of the NMR tube, then the optic fiber is pulled down by a few millimeters."

In addition, there are a few minor technical issues that need fixing in the final version of the paper. Fig1 legend, for panels D,E: it is mentioned "simulation of the absorbed power (AU)", and the graphs show "Absorption fraction" – what exactly these mean, how these were defined and calculated? Presumably, these parameters should depend on the optical density (OD) of the sample as well? What was the sample OD for these simulations? Needs clarifying, in the figure legend and/or in the Methods.

We thank Referee 2 for the careful reading; indeed, we did not well define what we meant by the absorbed light. We will put the following text in the caption of Figure 1:

"The absorption fraction is the light flux absorbed within the NMR active sample volume divided by the light flux incident on the tube bottom. The absorption is computed by the Raytracing software using the Beer-Lambert law, assuming a fluorescein concentration of 10 µM/l (0.10752 cm^{-1})"

Line 137 refers to Figure 2 – presumably should refer to Figure 3 instead.

We thank Referee 2 for careful reading, this has been corrected (See answer to Referee 1).

Also, in the phrase “sample measured from the top and the bottom,” – presumably Authors mean that the sample is illuminated from the top and the To re-word in the text, and also in the Figure 3 legend. To add the key to Figure 3 (for red/blue), and/or fix the wording in the figure legend regarding the colors.

We thank Referee 2 for noticying this mistake. We reworded the sentence as follows:
“The SNE is 74-fold and 60-fold when the sample is illuminated from the top and the bottom, respectively (Figure 3).”

We corrected the caption of figure 3:
“**Figure 3: A) SNE evolution with illumination time, with illumination from the top (red) and from the bottom (blue). B) signal intensity after 2 seconds of illumination from the top (red) and from the bottom (blue). The sample contained 30 µM tryptophan and 10 µM fluorescein, with oxygen-quenching enzymes, GOCAT, and glucose (see Material and Methods).”**

Line 154 – Reword statement “Such concentrations are on the low standard of typical fragment screening by NMR”

We reworded the statement:
“For comparison, in fragment screening with saturation transfer difference (STD) NMR screening, the ligand concentrations vary between 50 to 500 µM, and a measurement time of 15-60 min.”

Fig 3A – the Y scale shows raw signal intensity (with an unclear small initial value without any illumination), whereas the text refers to SNE values. Perhaps the SNE values should be plotted on the figure, versus illumination time, not intensities, for consistency.

We thank Referee 2 for noticing this mistake. We corrected the Figure.
“

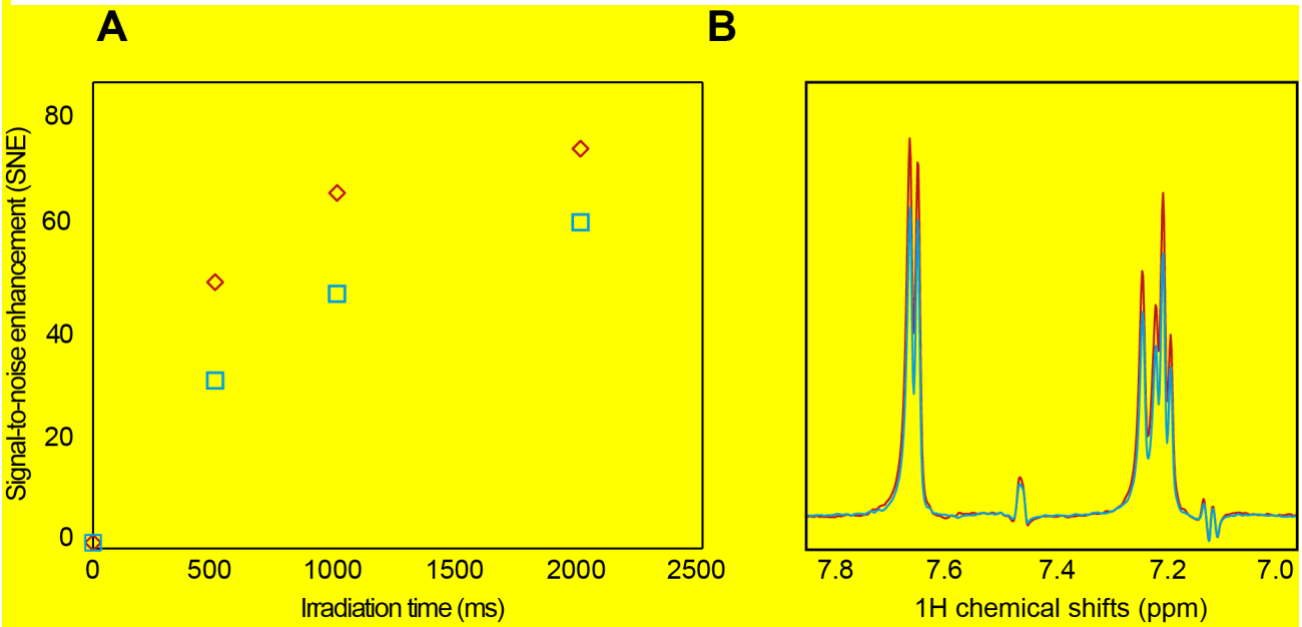

Figure 3: A) SNE evolution with illumination time, with illumination from the top (red) and from the bottom (blue). B) signal intensity after 2 seconds of illumination from the top (red) and from the bottom (blue). The sample contained 30 µM tryptophan and 10 µM fluorescein, with oxygen-quenching enzymes, GOCAT, and glucose (see Material and Methods).”

Line 200 – which cryoprobe exactly was used in the study? 5mm, or 3mm, what type exactly? Add information.
We thank Referee 2 for this question. We included in the material and method the cryoprobe we used to install our setup.

"All NMR measurements were performed at 298 K on a Bruker Avance III HD 600 MHz spectrometer equipped with a Bruker TCI 600 $^{1}H/^{13}C/^{15}N$ MHz CryoProbe."

As a very minor comment, it will help text readability if paragraphs in the text are separated with extra space between them and/or paragraph idents are used.

We thank Referee 2 for this suggestion. As we used the template from Magnetic Resonance Journal, we will comply with the requirements of the Editors on that particular matter.

Apart from these minor issues, the paper is easy to read and easy to follow, very nice work overall.